Int. J. Heat Mass Transfer. Vol. 36, No. 12, pp. 2957–2963, 1993
Printed in Great Britain

0017–9310/93 $6.00 + 0.00

Similarity solution for laminar film boiling over a moving isothermal surface

J. FILIPOVIC, R. VISKANTA and F. P. INCROPERA
Heat Transfer Laboratory, School of Mechanical Engineering, Purdue University, West Lafayette, IN 47907, U.S.A.

(*Received* 2 *September* 1992 *and in final form* 14 *January* 1993)

Abstract—Forced film boiling arises when a liquid flows over a highly superheated surface or when the surface moves through a liquid which is stationary or is itself in motion. As a result of the vapor layer separating the surface and the liquid, there is a significant reduction in the drag force and heat transfer. In this study, a similarity solution of the boundary layer equations is obtained, and for a wide range of subcooling parameters and surface velocities, related numerical results are shown to be in excellent agreement with predictions based on an integral method.

INTRODUCTION

FORCED film boiling arises when a liquid flows over a highly superheated surface or when the surface moves through a liquid which is stationary or is itself in motion. With a vapor layer separating the surface and the liquid, there is significant reduction in the drag force and heat transfer. In other words, the vapor layer acts as both a lubricant and an insulator. Besides quenching [1], which is very important in material processing, forced film boiling finds application in nuclear reactor safety [2] and drag reduction [3, 4].

Following Bromley *et al.* [5] and Motte and Bromley [6], who studied heat transfer from circular cylinders in forced-convective film boiling, a large number of investigators employed a variety of techniques to analyze film boiling for different geometries, such as the flat plate [7, 8], wedge [9] and sphere [10]. Among the theoretical studies, special mention should be made of the pioneering work by Cess and Sparrow [7, 8], who developed a two-phase boundary layer model. Using a combined analytical–numerical method, heat transfer and skin friction results were reported for laminar film boiling under saturated [7] and subcooled [8] conditions for a range of parameters of practical interest. A more detailed, numerical solution of the vapor and liquid boundary layer equations was obtained by Ito and Nishikawa [11], and good agreement was reported with the results of Cess and Sparrow [7, 8]. Retaining the assumption of two-phase boundary layer behavior, Nakayama and Koyama [12] applied an integral method to solve the set of the boundary layer equations and obtained good agreement with the results of Ito and Nishikawa [11].

In an attempt to further simplify the computational procedure, Chappidi *et al.* [13] proposed an analogy between conditions at the vapor–liquid interface and a surface moving in a single phase fluid. Previously developed expressions for single-phase flow over a moving surface were used with the vapor boundary layer equations and matching conditions at the vapor–liquid interface to obtain the skin friction and heat transfer. Although agreement between predicted results and those obtained from a numerical solution of the full set of model equations was very good for subcooled conditions, the method failed to predict accurately hydrodynamic and thermal behavior for saturated conditions.

Zumbrunnen *et al.* [1] analyzed heat transfer in laminar film boiling from a moving surface. They applied the integral method to solve the two-phase boundary layer equations and found that surface motion significantly increased heat transfer, even when the liquid was subcooled. A large increase in heat transfer was reported for concurrent liquid–surface motion, where the surface motion thins the vapor layer. On the other hand, if the liquid stream and plate move in opposite directions, which can occur, for example, in the accelerated cooling of a steel strip, heat transfer decreases due to an increase in the vapor layer thickness. Although it was stated that surface motion is especially important when the strip speed greatly exceeds the liquid velocity (the extreme case is for a quiescent liquid), it was not possible to determine the local Nusselt number from the model results. The local Reynolds number was based on the free stream velocity, which for this case was equal to zero.

The objectives of this study are (i) to obtain a similarity solution for laminar film boiling over a moving plate, (ii) to extend existing results [1] based on an integral solution (including the quiescent liquid case), and (iii) to compare the approximate and exact solutions of the model equations in order to check the accuracy of the integral solution.

THEORETICAL ANALYSIS

Physical model and assumptions

Consider flow of a liquid over a horizontal flat plate maintained at uniform temperature T_p, which is high

NOMENCLATURE

C_{fx}	local skin friction coefficient, $\tau_p/(1/2\rho_l u_i^2)$
c_p	specific heat at constant pressure [J kg^{-1} K^{-1}]
f	dimensionless stream function defined by equation (12)
h	heat transfer coefficient [W m^{-2} K^{-1}]
h_{fg}	latent heat of vaporization [J kg^{-1}]
Ja	Jakob number, $c_{pv}(T_p-T_s)/h_{fg}$
k	thermal conductivity [W m^{-1} K^{-1}]
$\dot{m}$	mass flow per unit width of plate [kg s^{-1} m^{-1}]
Nu_x	local Nusselt number, hx/k_v
Pr	Prandtl number, $\mu c_p/k$
q''	heat flux [W m^{-2}]
Re_x	local Reynolds number, $u_i x/\nu_l$
T	temperature [K]
u	x component of velocity [m s^{-1}]
u_i	the largest velocity in the system (if $u_\infty > v_p$, $u_i = u_\infty$; if $v_p > u_\infty$, $u_i = v_p$) [m s^{-1}]
u_s	x component of the interfacial velocity [m s^{-1}]
$\bar{u}_s$	dimensionless x component of the interfacial velocity, u_s/u_i
v	y component of velocity [m s^{-1}]
v_p	plate velocity [m s^{-1}]
$\bar{v}_p$	dimensionless plate velocity, v_p/u_i
x	streamwise coordinate [m]
y	vertical coordinate [m]
y_l	vertical position above vapor layer, $y-\delta_v$ [m]
Z	density viscosity product ratio, $\rho_l\mu_l/\rho_v\mu_v$.

Greek symbols

β	subcooling parameter, $Pr_v c_{pl}(T_s-T_\infty)/Pr_l c_{pv}(T_p-T_s)$
Γ	boundary layer thickness ratio, Δ/δ
δ	velocity boundary layer thickness in liquid [m]
δ_v	vapor layer thickness [m]
Δ	thermal boundary layer thickness in liquid [m]
η	similarity variable defined by equation (10)
θ_l	dimensionless liquid temperature, $(T_l-T_\infty)/(T_s-T_\infty)$
θ_v	dimensionless vapor temperature $(T_v-T_s)/(T_p-T_s)$
μ	dynamic viscosity [kg s^{-1} m^{-1}]
ν	kinematic viscosity [m^2 s^{-1}]
ρ	mass density [kg m^{-3}]
τ	shear stress [N m^{-2}]
φ	parameter defined by equation (26)
ψ	stream function defined by equation (11).

Subscripts

j	for vapor layer j = v and for liquid layer j = l
l	liquid
p	plate
s	vapor/liquid interface
v	vapor
∞	liquid free stream.

enough for boiling to occur and for a vapor layer to form adjacent to the surface (Fig. 1). The plate moves from left to right with a constant velocity v_p. The assumptions made in the analysis are that: (i) the flow is steady, (ii) the thermophysical properties are constant and uniform and are evaluated at the film temperature, T_f, (iii) the liquid–vapor interface is smooth, (iv) vapor formation and the liquid boundary layer start at $x = 0$, (v) the plate surface is impermeable and smooth, (vi) the body force is negligible in comparison to the viscous and inertial forces, and (vii) the effect of radiation on vapor layer formation is negligible.

The governing equations, compatibility and boundary conditions

With the simplifying assumptions outlined above, the governing equations [11] are

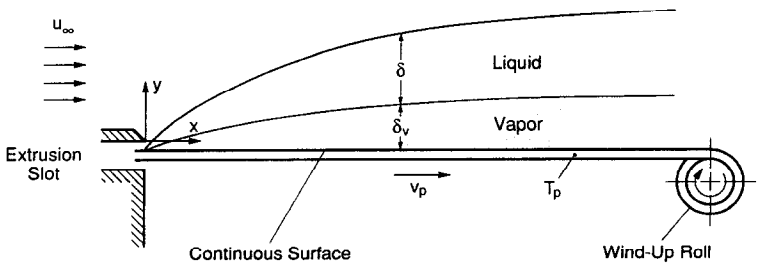

FIG. 1. Schematic of the physical model and coordinate system.

$$\frac{\partial u_j}{\partial x}+\frac{\partial v_j}{\partial y}=0 \tag{1}$$

$$u_j\frac{\partial u_j}{\partial x}+v_j\frac{\partial u_j}{\partial y}=\nu_j\frac{\partial^2 u_j}{\partial y^2} \tag{2}$$

$$u_j\frac{\partial T_j}{\partial x}+v_j\frac{\partial T_j}{\partial y}=\alpha_j\frac{\partial^2 Y_j}{\partial y^2} \tag{3}$$

where for the vapor layer $j=\mathrm{v}$ and for the liquid layer $j=\mathrm{l}$. The boundary conditions are:

$$y=0:\quad u_\mathrm{v}=v_\mathrm{p},\quad v_\mathrm{v}=0,\quad T_\mathrm{v}=T_\mathrm{p} \tag{4}$$

$$y=\delta_\mathrm{v}:\quad u_\mathrm{v}=u_\mathrm{l}=u_\mathrm{s},\quad T_\mathrm{v}=T_\mathrm{l}=T_\mathrm{s} \tag{5}$$

$$y\to\infty:\quad u_\mathrm{l}=u_\infty,\quad T_\mathrm{l}=T_\infty. \tag{6}$$

Conservation of mass at the vapor–liquid interface ($y=\delta_\mathrm{v}$) requires that

$$\dot{m}=\rho_\mathrm{v}\left(u_\mathrm{v}\frac{\mathrm{d}\delta_\mathrm{v}}{\mathrm{d}x}-v_\mathrm{v}\right)=\rho_\mathrm{l}\left(u_\mathrm{l}\frac{\mathrm{d}\delta_\mathrm{v}}{\mathrm{d}x}-v_\mathrm{l}\right). \tag{7}$$

The compatibility condition for the shear stress at the interface ($y=\delta_\mathrm{v}$) is given by

$$\mu_\mathrm{v}\frac{\partial u_\mathrm{v}}{\partial y}=\mu_\mathrm{l}\frac{\partial u_\mathrm{l}}{\partial y} \tag{8}$$

and the corresponding energy balance can be expressed

$$\dot{m}h_\mathrm{fg}=-k_\mathrm{v}\frac{\partial T_\mathrm{v}}{\partial y}+k_\mathrm{l}\frac{\partial T_\mathrm{l}}{\partial y}. \tag{9}$$

Similarity solution

A solution of the model equations can be obtained using a similarity transformation. We introduce similarity variables which reduce the set of partial differential equations to a set of ordinary differential equations. The similarity variables for vapor and liquid layers are defined as

$$\eta_\mathrm{v}=y\sqrt{(u_\mathrm{i}/\nu_\mathrm{v}x)}\quad\text{and}\quad\eta_\mathrm{l}=(y-\delta_\mathrm{v})\sqrt{(u_\mathrm{i}/\nu_\mathrm{l}x)} \tag{10}$$

where, for $u_\infty>v_\mathrm{p}$, $u_\mathrm{i}=u_\infty$, and for $v_\mathrm{p}>u_\infty$, $u_\mathrm{i}=v_\mathrm{p}$.

The velocity components, defined in terms of stream functions ψ_v and ψ_l, are given by

$$u_j=\frac{\partial\psi_j}{\partial y}\quad\text{and}\quad v_j=-\frac{\partial\psi_j}{\partial x}. \tag{11}$$

In terms of the dimensionless stream function,

$$f_j(\eta_j)=\psi_j/\sqrt{(u_\mathrm{i}\nu_j x)} \tag{12}$$

the velocity components u_j and v_j become

$$u_j=u_\mathrm{i}f'_j(\eta_j)\quad\text{and}\quad v_j=1/2(u_\mathrm{i}\nu_j/x)^{1/2}(\eta_j f'_j-f_j). \tag{13}$$

Introducing the similarity and dimensionless variables into the model equations (1)–(3), we obtain the following equations

$$2f'''_j+f_jf''_j=0 \tag{14}$$

$$2\theta''_j+Pr_jf_j\theta'_j=0. \tag{15}$$

The boundary conditions given by equations (4)–(6) now become:

$$\eta_\mathrm{v}=0:\quad f'_\mathrm{v}(0)=\frac{v_\mathrm{p}}{u_\mathrm{i}},\quad f_\mathrm{v}(0)=0,\quad\theta_\mathrm{v}(0)=1 \tag{16}$$

$$\eta_\mathrm{l}=0:\quad f'_\mathrm{v}(\eta_\mathrm{v})_\mathrm{s}=f'_\mathrm{l}(0)=\frac{u_\mathrm{s}}{u_\mathrm{i}},$$

$$\theta_\mathrm{v}(\eta_\mathrm{v})_\mathrm{s}=0,\quad\theta_\mathrm{l}(0)=1 \tag{17}$$

$$\eta_\mathrm{l}\to\infty:\quad f'_\mathrm{l}(\infty)=\frac{u_\infty}{u_\mathrm{i}},\quad\theta_\mathrm{l}(\infty)=0. \tag{18}$$

Similarly, the interface ($y=\delta_\mathrm{v}$) compatibility conditions, equations (7)–(9), become, respectively,

$$(f_\mathrm{l})_\mathrm{s}=Z^{-1/2}(f_\mathrm{v})_\mathrm{s} \tag{19}$$

$$(f'_\mathrm{l})_\mathrm{s}=Z^{-1/2}(f''_\mathrm{v})_\mathrm{s} \tag{20}$$

$$\beta(\theta'_\mathrm{l})_\mathrm{s}Z^{1/2}-(\theta'_\mathrm{v})_\mathrm{s}=Pr_\mathrm{v}(f_\mathrm{v})_\mathrm{s}/2Ja. \tag{21}$$

The local skin friction coefficient can be expressed in terms of dimensionless parameters as

$$C_{\mathrm{f},x}=\tau_\mathrm{p}/(1/2\rho_\mathrm{l}u_\mathrm{i}^2)=2Z^{-1/2}|f''_\mathrm{v}(0)|Re_x^{-1/2}. \tag{22}$$

The local Nusselt number based on the plate superheat and vapor thermal conductivity is given by

$$Nu_x=\frac{q''x}{k_\mathrm{v}(T_\mathrm{p}-T_\mathrm{s})}=-\frac{\mu_\mathrm{l}}{\mu_\mathrm{v}}Z^{-1/2}(\theta'_\mathrm{v})_0Re_x^{1/2}. \tag{23}$$

Solution procedure

The transformed governing equations (14) and (15) were solved numerically using the fourth order Runge–Kutta method with a shooting procedure to find the missing interface (from the liquid side) and wall shear stress. By prescribing the dimensionless interface velocity, $\bar{u}_\mathrm{s}$, and vapor layer thickness, $(\eta_\mathrm{v})_\mathrm{s}$, together with the parameters Pr_l, Pr_v, Ja and Z, the momentum equations were solved to satisfy the boundary and matching conditions. The dimensionless velocity distributions were then used to obtain the dimensionless temperature distributions. Using the calculated wall velocity and temperature gradients, the local skin friction coefficient and Nusselt number were determined. Finally, the subcooling parameter, β, was calculated from equation (21). The step size used in the liquid layer was $\Delta\eta_\mathrm{l}=0.2$, and the free stream boundary conditions at infinity were satisfied with an accuracy of order $\varepsilon=10^{-6}$. Forty grid points were used in the vapor layer. Increasing the number of grid points from 40 to 80 did not affect results for the skin friction and heat transfer. The calculation procedure was validated through comparison with the results of Chappidi *et al.* [13] for flow and heat transfer over a stationary plate.

Integral method

Extending the integral approach of Zumbrunnen *et al.* [1] to include conditions for which the plate moves

through a quiescent fluid, all velocities appearing in the appropriate equations are nondimensionalized by the highest velocity in the system. That is, if the free stream velocity exceeds the plate velocity, $u_\infty > v_p$, it serves as the reference velocity ($u_i = u_\infty$). Similarly, if $v_p > u_\infty$, $u_i = v_p$. Also, the Reynolds number is based on the highest velocity. In this way all possible cases are considered, including a stagnant ambient fluid for which $u_\infty = 0$. Linear velocity and temperature distributions were assumed for the vapor layer, while second order polynomials were prescribed for the liquid layer. For a comprehensive discussion of the procedure, including the governing equations, assumptions and boundary conditions, the reader is referred to Zumbrunnen *et al.* [1].

To determine the dimensionless interfacial velocity, $\bar{u}_s$, the following system of equations, which results from the interfacial energy balance and the liquid layer energy equation,

$$\frac{\Gamma Pr_l}{8\varphi} = \left[2(\bar{u}_\infty - \bar{u}_s)\Gamma^2(5-\Gamma) + 20\Gamma\bar{u}_s + \frac{15}{Z}\frac{(\bar{u}_s^2 - \bar{v}_p^2)}{(\bar{u}_\infty - \bar{u}_s)}\right]^{-1} \quad (24)$$

$$\frac{15}{8\varphi}\frac{Pr_v}{JaZ}(\bar{u}_s + \bar{v}_p)\left[\frac{\bar{u}_s - \bar{v}_p}{\bar{u}_\infty - \bar{u}_s}\right]^2 = 1 - \frac{\beta(\bar{u}_s - \bar{v}_p)}{\Gamma(\bar{u}_\infty - \bar{u}_s)} \quad (25)$$

where

$$\varphi = \bar{u}_\infty + 3/2\bar{u}_s + \frac{15}{8Z}\frac{(\bar{u}_s^2 - \bar{v}_p^2)}{(\bar{u}_\infty - \bar{u}_s)} \quad (26)$$

was solved.

The ratio of the vapor layer thickness to the liquid boundary layer thickness is found to be

$$\frac{\delta_v}{\delta} = \frac{\mu_v}{2\mu_l}\frac{(\bar{u}_s - \bar{v}_p)}{(\bar{u}_\infty - \bar{u}_s)} \quad (27)$$

where

$$\delta(x) = x(30/\varphi)^{1/2}Re_x^{-1/2}. \quad (28)$$

The local skin friction coefficient can be expressed as

$$C_{f,x} = \tau_p(1/2\rho_l u_i^2) = 4|\bar{u}_\infty - \bar{u}_s|\left(\frac{\varphi}{30}\right)^{1/2}Re_x^{-1/2}. \quad (29)$$

The resulting equation for the local Nusselt number is

$$Nu_x = \frac{q''x}{k_v(T_p - T_s)} = \frac{\mu_l}{\mu_v}\left(\frac{2\varphi}{15}\right)^{1/2}\frac{(\bar{u}_\infty - \bar{u}_s)}{(\bar{u}_s - \bar{v}_p)}Re_x^{1/2}. \quad (30)$$

It is of interest to consider special cases corresponding to saturated and highly subcooled liquids. Using equation (25), with $\beta = 0$ (saturated conditions) and $\bar{v}_p = 0$, the local skin friction coefficient (equation (29)) becomes

$$C_{f,x} = [Pr_v/JaZ]^{1/2}Re_x^{-1/2}. \quad (31)$$

Similarly, for the local Nusselt number we obtain

$$Nu_x = 1/2\mu_l/\mu_v[Pr_v/JaZ]^{1/2}Re_x^{1/2}. \quad (32)$$

For highly subcooled liquids with $\bar{v}_p = 0$ and $Pr_l = 1$ the following expressions were obtained

$$C_{f,x} = 2(2/15)^{1/2}Re_x^{-1/2} \quad (33)$$

$$Nu_x = \mu_l/\mu_v(2/15)^{1/2}\beta Re_x^{1/2}. \quad (34)$$

Also, for highly subcooled liquids with $\bar{v}_p = 0$ and $Pr_l \ll 1$, we obtain

$$Nu_x = \mu_l/\mu_v(1/3)^{1/2}\beta Re_x^{1/2} \quad (35)$$

while the local skin friction coefficient was independent of Pr_l. Equations (31) and (32) are exactly the same as those derived by Cess and Sparrow [7], while equations (33), (34) and (35) correspond to those obtained by Nakayama and Koyama [12]. The value of the constant in equation (35) is very close to that appearing in the expression for the local Nusselt number obtained by Cess and Sparrow [8] ($(1/3)^{1/2} = 0.577 \approx (1/\pi)^{1/2} = 0.564$).

In the limit as the thickness of the vapor layer approaches zero, the vapor/liquid interface coincides with the plate surface. Hence, from equation (27), the interfacial velocity equals the plate velocity ($\bar{u}_s = \bar{v}_p$), and vapor layer equations are no longer pertinent. Moreover, for $\bar{v}_p = 0$ (stationary plate), single phase equations for δ, $C_{f,x}$ [14] and Nu_x are recovered.

RESULTS AND DISCUSSION

Results for the dimensionless interfacial velocity, the liquid layer velocity and temperature profiles, and the local skin friction coefficient and Nusselt number are given in Figs. 2–10 for a range of subcooling parameters β and plate velocities v_p for both $u_\infty > v_p$ and $v_p > u_\infty$. The results correspond to fixed values of $Pr_l = 2.5$, $Pr_v = 1.0$, $Ja = 0.1$ and $Z = 47\,620$.

Velocity and temperature distributions

Figures 2 and 3 show the variation of the dimensionless interfacial velocity $\bar{u}_s$ with β for $u_\infty > v_p$ and

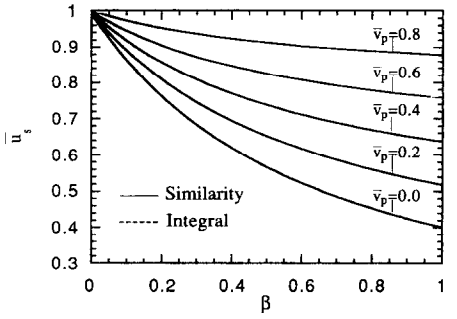

FIG. 2. Variation of the dimensionless interfacial velocity with β for $u_\infty > v_p$.

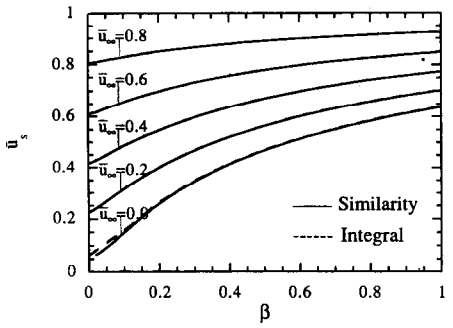

FIG. 3. Variation of the dimensionless interfacial velocity with β for $v_p > u_\infty$.

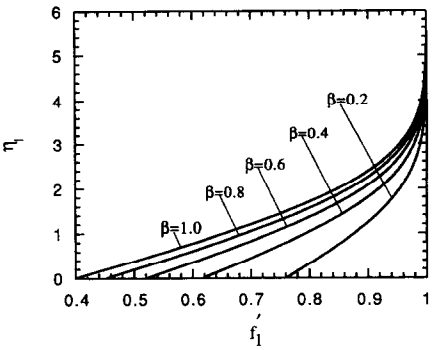

FIG. 4. Influence of subcooling on the dimensionless liquid velocity distribution for $v_p = 0$.

$v_p > u_\infty$, respectively. Clearly, the similarity and integral results are in excellent agreement.

The family of curves for different $\bar{v}_p$ in Fig. 2 reveals that, for $u_\infty > v_p$, the interfacial velocity decreases with increasing subcooling parameter and decreasing plate velocity. This trend may be confirmed by referring to equations (24) and (25) and assuming, for the sake of simplicity that, $Pr_l = 1$ ($\Gamma = 1$) and that $Z \gg 1$. The second assumption is certainly realistic for water in typical quenching applications, where $Z \approx 40\,000$. For these conditions the following simple expression is obtained for the dimensionless interfacial velocity,

$$\bar{u}_s = (\bar{u}_\infty + \beta\bar{v}_p)/(1+\beta). \tag{36}$$

If $u_\infty > u_p$, $\bar{u}_\infty = 1$, and since $0 \leqslant \bar{v}_p \leqslant 1$, it follows that, with increasing β, the term $(1+\beta)$ increases faster than $1+\beta\bar{v}_p$. On the other hand, when $\bar{v}_p$ increases, $\bar{u}_s$ also increases.

When the plate moves faster than the free stream ($v_p > u_\infty$), the trend is different (Fig. 3). As equation (36) suggests, when $\bar{v}_p = 1$, $\bar{u}_s$ increases with increasing β and $\bar{u}_\infty$.

The physical basis of the foregoing trends is tied to the influence of subcooling on the thickness of the vapor layer. Namely, if subcooling increases the thickness of the vapor layer is reduced and the interface is closer to the plate. Hence, if $u_\infty > v_p$, the interface velocity decreases due to increasing drag force imposed by the plate. If the plate velocity is increased, these effects become less severe, and the interface velocity increases. When the plate moves faster than the free stream ($v_p > u_\infty$), the effects of subcooling on the vapor layer thickness remain unchanged, but the interfacial velocity increases with increasing subcooling. Interface motion is now restrained by the free stream, and because δ_v decreases with increasing β, the interface becomes further removed from the free stream, thereby decreasing the restraining influence. The effect of increasing free stream velocity on the interfacial velocity is similar to that of increasing plate velocity for $u_\infty > v_p$.

Figure 4 shows the influence of subcooling on the dimensionless liquid velocity distribution for $v_p = 0$. Similar trends were obtained for $v_p > 0$, except that the interfacial velocities are higher. The velocity profiles are strongly influenced by the magnitude of the dimensionless interfacial velocity, revealing the analogy with single-phase flow over a plate moving with velocity equal u_s. With decreasing β, u_s increases (see equation (32)), while the difference between the free stream velocity and interfacial velocity decreases, approaching zero as saturation conditions are approached ($\beta \to 0$). For saturated conditions, $u_s = u_\infty$ and the liquid boundary layer is eliminated. On the other hand, when β tends to infinity, $u_s \to v_p$ and the flow attains single-phase conditions.

As Fig. 5 shows, the influence of subcooling on the dimensionless liquid velocity distribution for $u_\infty = 0$ is similar to that for $v_p = 0$. Although the interfacial velocity decreases with decreasing subcooling, the absolute value of the difference between the free stream velocity and interfacial velocity also decreases. The influence of subcooling on the dimensionless liquid temperature distribution for $v_p = 0$ is shown in Fig. 6. The dimensionless liquid temperature distributions for $u_\infty = 0$ are very similar to those for $v_p = 0$ and are therefore not included. Moreover, in all cases the dimensionless vapor velocity and temperature distributions were extremely linear.

Skin friction and heat transfer

The local skin friction coefficient results are shown in Figs. 7 and 8. For $v_p > u_\infty$ (Fig. 8), the similarity

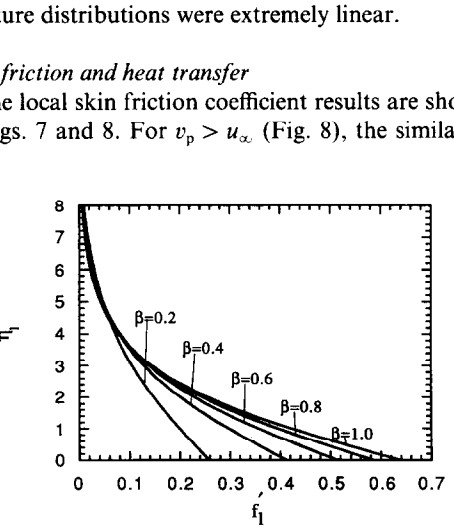

FIG. 5. Influence of subcooling on the dimensionless liquid velocity distribution for $u_\infty = 0$.

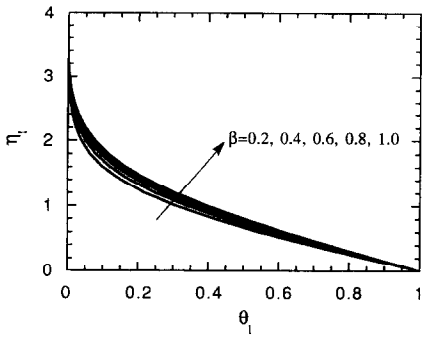

FIG. 6. Influence of subcooling on the dimensionless liquid temperature distribution for $v_p = 0$.

and integral results are almost indistinguishable, while for $u_\infty > v_p$ (Fig. 7) the agreement is within 2.6% ($\bar{v}_p = 0.8$) and 4.2% ($\bar{v}_p = 0$). For both $u_\infty > v_p$ and $v_p > u_\infty$, the skin friction coefficient increases with increasing β. With increasing β, a larger fraction of the heat extracted from the plate is transferred to the subcooled liquid, and a smaller fraction is consumed in vapor generation. Hence, the vapor layer is thinned, and its frictional resistance is increased. It is interesting to note that for $v_p > u_\infty$ and for smaller values of β, C_{fx} is smaller for $\bar{u}_\infty = 0$ than for $\bar{u}_\infty = 0.2$, 0.4 and 0.6. The behavior was predicted by both the similarity and integral methods and values of β for which crossover occurs may be obtained by equating expressions for C_{fx} corresponding to $\bar{u}_\infty = 0$ on the one hand and $\bar{u}_\infty = 0.2$, 0.4 or 0.6 on the other. Analyzing equation (29), we see that the local skin friction coefficient, C_{fx}, is proportional to the dimensionless relative velocity between the free stream and interface, $|\bar{u}_\infty - \bar{u}_s|$, and inversely proportional to the velocity boundary layer thickness in the liquid, δ. For smaller values of β, the velocity boundary layer thickness in the liquid, $\delta \approx (\bar{u}_\infty + 3/2\bar{u}_s)^{-1/2}$, decreases with both β and $\bar{u}_\infty$ (or $\bar{u}_s$) and is the dominant parameter. In other words, the rate at which δ decreases with increasing $\bar{u}_\infty$ is larger than the rate at which $|\bar{u}_\infty - \bar{u}_s|$ decreases. Hence, C_{fx}, which is proportional to the ratio of $|\bar{u}_\infty - \bar{u}_s|$ to δ, is larger for $\bar{u}_\infty = 0.2$, 0.4 and 0.6 than for $\bar{u}_\infty = 0$.

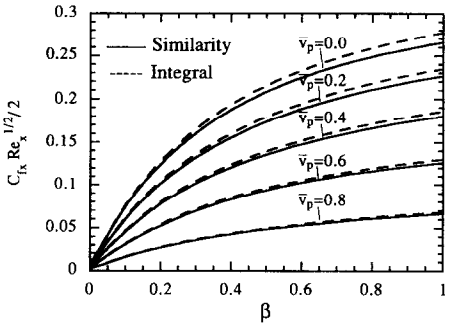

FIG. 7. Skin friction results for $u_\infty > v_p$.

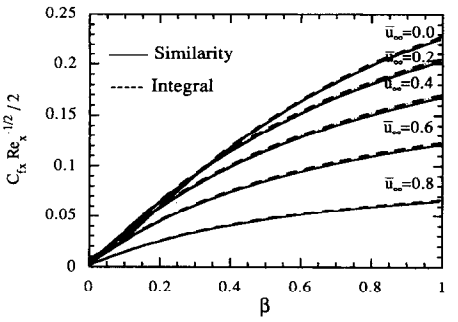

FIG. 8. Skin friction results for $v_p > u_\infty$.

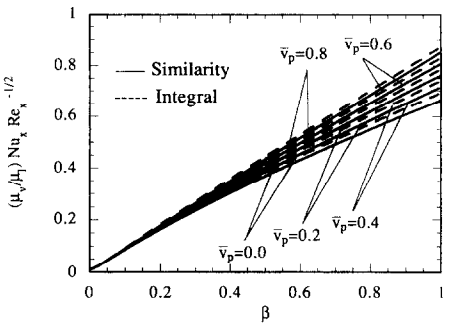

FIG. 9. Heat transfer results for $u_\infty > v_p$.

Figures 9 and 10 show the dependence of local Nusselt number on β, with either $\bar{v}_p$ or $\bar{u}_\infty$ as a parameter. For $u_\infty > v_p$ (Fig. 9), the largest discrepancy between the similarity and integral results is 4.1% ($\bar{v}_p = 0$ and $\beta = 1$), and for $v_p > u_\infty$ it is 3.1% ($\bar{u}_\infty = 0.8$ and $\beta = 1$). In both cases Nu_x increases with increasing subcooling. This behavior is due to thinning of the vapor layer, which acts as an insulator between the plate and liquid. Similarly, the vapor layer is thinned with increasing $\bar{v}_p$ or $\bar{u}_\infty$, thereby increasing heat transfer. Note that the dependence of the local Nusselt number on a ratio of plate and freestream velocities indicates that, if either u_∞ or v_p is fixed, the other velocity may be selected to maximize heat transfer. The results of Figs. 9 and 10 can be used for all values of the two velocities in the subcooling parameter range ($0 < \beta < 1$) and include as an important special case, $\bar{u}_\infty = 0$.

CONCLUSIONS

The similarity and integral results for skin friction and heat transfer for forced film boiling over a moving

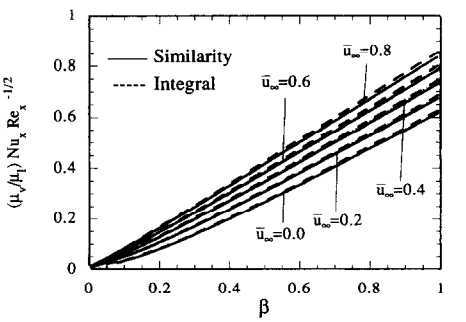

FIG. 10. Heat transfer results for $v_p > u_\infty$.

isothermal plate are in excellent agreement. Owing to this agreement, the integral method can be used with confidence and all the additional assumptions and further simplifications can be tested against the similarity solution. The results are presented in a manner that enables optimization of heat transfer in terms of the ratio of the flow to the plate velocity. The ability to determine heat transfer from a plate moving through a quiescent liquid also exists. Application of the results requires information about the critical Reynolds number for transition to turbulence. In order to gain confidence in the predictions, experimental data are needed for model validation.

Acknowledgements—This work was supported by the National Science Foundation under Grant CTS-8912831.

REFERENCES

1. D. A. Zumbrunnen, R. Viskanta and F. P. Incropera, The effect of surface motion on forced convection film boiling heat transfer, *ASME J. Heat Transfer* **111,** 760–766 (1989).
2. F. S. Gunnerson and J. A. Meyer, An investigation of boiling behavior with applications to nuclear reactor safety, UCF Report No. 16-26-805 (1987).
3. W. S. Bradfield, R. O. Barkdoll and J. T. Byrne, Some effects of boiling on hydrodynamic drag, *Int. J. Heat Mass Transfer* **5,** 615–622 (1962).
4. A. Gay, Film boiling heat transfer and drag reduction, Convair Aerospace Division Report, San Diego, California, GDCA-DDB-71-001 (1973).
5. L. A. Bromley, N. R. Leroy and J. A. Robbers, Heat transfer in forced convection film boiling, *Ind. Engng Chem.* **45,** 2639–2646 (1953).
6. E. I. Motte and L. A. Bromley, Film boiling of flowing subcooled liquids, *Ind. Engng Chem.* **49,** 1921–1928 (1957).
7. R. D. Cess and E. M. Sparrow, Film boiling in a forced convection boundary layer flow, *ASME J. Heat Transfer* **83,** 370–376 (1961).
8. R. D. Cess and E. M. Sparrow, Subcooled forced convection film boiling on a flat plate, *ASME J. Heat Transfer* **83,** 377–379 (1961).
9. A. Nakayama, Subcooled forced-convection film boiling in presence of a pressure gradient, *AIAA Journal* **24,** 230–236 (1986).
10. K. Kobayasi, Film boiling heat transfer around a sphere in forced convection, *J. Nucl. Sci. Tech.* **2,** 62–67 (1965).
11. S. Ito and K. Nishikawa, Two-phase boundary layer treatment of forced convection film boiling, *Int. J. Heat Mass Transfer* **9,** 117–130 (1966).
12. A. Nakayama and H. Koyama, Integral treatment of subcooled forced convection film boiling on a flat plate, *Wärme- und Stoffübertragung* **20,** 121–126 (1986).
13. P. R. Chappidi, F. S. Gunnerson and K. O. Pasamehmetoglu, A simple forced convection film boiling model, *Int. Com. Heat Mass Transfer* **17,** 259–270 (1990).
14. R. W. Fox and A. T. McDonald. In *Introduction to Fluid Mechanics*, Chap. 8. Wiley, New York (1973).